



## King's Research Portal

DOI:

[10.1021/acs.langmuir.6b03367](https://doi.org/10.1021/acs.langmuir.6b03367)

*Document Version*

Peer reviewed version

[Link to publication record in King's Research Portal](#)

*Citation for published version (APA):*

Valero, M., Castiglione, F., Mele, A., Da Silva, M. A., Grillo, I., González-Gaitano, G., & Dreiss, C. A. (2016). Competitive and Synergistic Interactions between Polymer Micelles, Drugs, and Cyclodextrins: The Importance of Drug Solubilization Locus. *Langmuir : the ACS journal of surfaces and colloids*, 32(49), 13174-13186. <https://doi.org/10.1021/acs.langmuir.6b03367>

### **Citing this paper**

Please note that where the full-text provided on King's Research Portal is the Author Accepted Manuscript or Post-Print version this may differ from the final Published version. If citing, it is advised that you check and use the publisher's definitive version for pagination, volume/issue, and date of publication details. And where the final published version is provided on the Research Portal, if citing you are again advised to check the publisher's website for any subsequent corrections.

### **General rights**

Copyright and moral rights for the publications made accessible in the Research Portal are retained by the authors and/or other copyright owners and it is a condition of accessing publications that users recognize and abide by the legal requirements associated with these rights.

- Users may download and print one copy of any publication from the Research Portal for the purpose of private study or research.
- You may not further distribute the material or use it for any profit-making activity or commercial gain
- You may freely distribute the URL identifying the publication in the Research Portal

### **Take down policy**

If you believe that this document breaches copyright please contact [librarypure@kcl.ac.uk](mailto:librarypure@kcl.ac.uk) providing details, and we will remove access to the work immediately and investigate your claim.

# Competitive and synergistic interactions between polymer micelles, drugs, and cyclodextrins: the importance of drug solubilisation locus

Margarita Valero,<sup>\*,a</sup> Franca Castiglione,<sup>b</sup> Andrea Mele,<sup>b</sup> Marcelo A. da Silva,<sup>c</sup> I. Grillo,  
Gustavo González-Gaitano,<sup>d</sup> Cécile A. Dreiss<sup>\*,c</sup>

<sup>a</sup>Dpto. Química Física, Facultad de Farmacia, Universidad de Salamanca, Campus Miguel de Unamuno, s/n, 37007 Salamanca, Spain

<sup>b</sup> Department of Chemistry, Materials and Chemical Engineering “G. Natta”, Politecnico di Milano, Piazza L. Da Vinci 32 I-20133, Milano, Italy

<sup>c</sup> Institute of Pharmaceutical Science, King’s College London, Franklin-Wilkins Building, 150 Stamford Street, London SE1 9NH, U.K.

<sup>d</sup>Departamento de Química, Universidad de Navarra, 31080 Pamplona, Spain

\*Corresponding authors: mvalero@usal.es; cecile.dreiss@kcl.ac.uk

## Abstract

Polymeric micelles, in particular PEO-PPO-based Pluronic, have emerged as promising drug carriers, while cyclodextrins, cyclic oligosaccharides with an apolar cavity, have long been used for their capacity to form inclusion complexes with drugs. Dimethylated  $\beta$ -cyclodextrin (CD) has the capacity to fully break-up F127 Pluronic micelles, while this effect is substantially hindered if drugs are loaded within the micellar aggregates. Four drugs were studied at physiological temperature: lidocaine (LD), pentobarbital sodium salt (PB), sodium naproxen (NP), and sodium salicylate (SAL); higher temperatures shift the equilibrium towards higher drug partitioning and lower drug:CD binding compared to 25°C.<sup>1</sup> The impact of drugs on micellar structure was characterised by small-angle neutron scattering (SANS), while their solubilisation locus was revealed by 2D NOESY NMR. UV and fluorescence spectroscopy, Dynamic and Static Light Scattering were employed to measure a range of micellar properties and drug:CD interactions: binding constant, drug partitioning within the micelles, critical micellar concentration of the loaded micelles, aggregation number ( $N_{agg}$ ). Critically, time-resolved SANS (TR-SANS) reveal that micellar break-up in the presence of drugs is substantially slower (100s of seconds) than for the free micelles (< 100 ms).<sup>2</sup> These results combined together give new insights into the mechanisms of protection of the drugs against CD-induced micellar break-up. The outcomes are practical guidelines to improve the design of drug delivery systems as well as an improved understanding of competitive assembly mechanisms leading to shape and function modulation.

## Introduction

Pluronic micelles, comprising a central poly(propylene oxide) (PPO) block flanked by two poly(ethylene oxide) (PEO) blocks, are emerging promising drug carrier candidates, particularly in the cancer arena.<sup>3-5</sup> They meet a number of key requirements as effective therapeutic agents: a distinct core-shell architecture providing physical entrapment of hydrophobic drugs, while reducing recognition by macrophages with their hydrophilic PEO corona; preferential accumulation within tumours and enhanced permeability and retention (EPR effect); inhibition of drug efflux pumps involved in multi-drug resistance.<sup>5</sup> Pluronic-based micellar formulation of the anticancer drug Dox, SP1049C, was the first polymeric micelle drug to advance to clinical stage, successfully completing phase II clinical trial in advanced oesophageal cancer patients.<sup>5, 6</sup>

While the positive features of Pluronics as drug carriers have long been recognised, and current clinical trials are demonstrating efficiency and safety, their potential still needs to be fully realised. A key issue in the realisation of this potential is the lack of understanding of structure-property relationships, in particular: how a specific drug structure relates to its solubilisation within a specific micellar architecture, and ultimately its release from the carrier. We have previously investigated the structure of Pluronic F127 micelles when loaded with drugs of different structure, showing substantial changes to micellar size depending on the nature of the loaded drug,<sup>1, 7</sup> in agreement with other reports;<sup>8, 9</sup> however, the rules that govern the loading ability of the micelle or the effect of the drug on the structure of the micelle are a long way from being established. For instance, it has been suggested that the partitioning of aromatic compounds into Pluronic micelles is strongly favoured,<sup>10</sup> while the presence of charge strongly limits their partitioning.<sup>1</sup>

In addition to drug-micelles interactions, our interest over the last few years has focused on ternary systems where cyclodextrins (CD) are present, which can both bind the drugs (forming an inclusion complex) and interact with the polymer, leading to interesting competitive interactions. CDs are cyclic oligosaccharides of conic shape, with a hydrophilic exterior and a relatively hydrophobic internal cavity, widely used in the pharmaceutical industry to solubilise lipophilic drugs.<sup>11</sup> Their interaction with polymers or amphiphiles can lead to a range of supramolecular structures that have been widely reviewed in the literature.<sup>12, 13</sup> Dimethylated  $\beta$ -cyclodextrin (DIMEB) - which has two hydrogens substituted by a methyl group on each glucose unit - interacts with Pluronic micelles by hindering micellisation, breaking them up completely at high

DIMEB/Pluronic ratio.<sup>1, 2, 7</sup> This destructive interaction is surprisingly selective and is not observed (or much reduced) with other CD derivatives.<sup>7</sup> The demicellisation induced by DIMEB – probably linked to an optimum balance between hydrophobicity and hydrogen-bonding ability - seems to be quite a generic feature of this cyclodextrin, as recently shown for X-shaped PEO-PPO block copolymers (poloxamines or Tetronics).<sup>14, 15</sup> This selective interaction is thus envisaged for the controlled release of drugs in specific body compartments.<sup>1</sup> Interestingly, the extent of this effect is not only controlled by composition (DIMEB/F127) ratio but also strongly dependent on the nature of the loaded drug: some drugs hinder DIMEB disruptive effect (thus ‘protecting’ the micelles), but to varying extents; the mechanisms, however, are not understood.<sup>2, 16</sup>

The current study focuses on physiological temperature (37°C). Not only is this temperature more relevant to drug studies, but by increasing the temperature several changes occur: micellisation is enhanced, drug partitioning increases,<sup>17, 18</sup> while drug:CD binding generally decreases. These changes in the balance of interactions give us a useful handle to gain new insights into the mechanisms, by contrasting and comparing to the situation at room temperature.<sup>1</sup> An important aspect of drug delivery systems (DDS) is the localization of the drugs within the aggregates; the locus of solubilisation is expected to correlate with important features such as drug loading and release rate from the aggregates.<sup>19</sup> Despite being such a key property, the drug solubilisation locus is usually unknown and scarcely studied. We report here 2D NMR data that provide information on drug localization, and which are then correlated with micellar structural features and drug partitioning.

This work focuses on the four drugs previously studied (**Scheme 1**): lidocaine (LD), pentobarbital (PB), salicylate (SAL) and naproxen (NP); the first is uncharged while the latter three are in their sodium salts, thus charged (at natural pH), and present different sizes of the polar and apolar regions. We use spectroscopic techniques (UV, fluorescence, NMR) in combination with static (SLS) and dynamic light scattering (DLS), small-angle neutron scattering (SANS) and time-resolved-SANS (TR-SANS), to examine the following aspects: the effect of drug loading on micellar structure and micellar properties; the partitioning of the drugs inside the micelles and their localization; the binding of the drugs to DIMEB, the critical micellar concentration, and the kinetics of micellar rupture. These results are then combined to discuss the mechanisms of protection of the drugs against DIMEB-induced micellar break-up.

## Experimental section

### Materials

Pluronic copolymer F127 comprising a central block of 65 PPO units and two side-blocks of PEO (100 units each) was obtained from Sigma-Aldrich UK ( $M_w = 12,600$ ). Heptakis(2,6-di-*O*-methyl)- $\beta$ -cyclodextrin (DIMEB) was obtained from Sigma-Aldrich UK (H0513,  $M_w = 1331.4 \text{ g mol}^{-1}$ ).

The drugs naproxen sodium salt (NP, M1275), pentobarbital sodium salt (PB, P3761), sodium salicylate (SAL, 71945) and lidocaine (LD, L7757) were purchased from Sigma Aldrich (Scheme 1). Methyl Orange (MO) was purchased from Panreac. All materials were used as received.

### Sample Preparation

Aqueous stock solutions of (1) drug alone, (2) drug/F127, and (3) drug/DIMEB, as well as combined (4) drug/F127/DIMEB were prepared by weight. For partition coefficient determination, solutions of different F127 concentrations were prepared by mixing the appropriate amount of solutions (1) and (2). For the determination of drug:CD binding constants in the absence and the presence of F127, solutions (3) and (1) were mixed with (4) and (2), respectively. In the case of lidocaine (the only one not in salt-form), the solutions were heated above the drug melting point ( $68^\circ\text{C}$ ) to facilitate diffusion and solubilisation into the micellar core. The solutions were then cooled back to room temperature.

For the determination of the critical micellar concentration (cmc), solutions (1) and (2) were prepared in MO/H<sub>2</sub>O ( $4 \times 10^{-5} \text{ M}$ ), with and without drug for loaded and free micelles respectively. A range of F127 concentrations were obtained by mixing varying amounts of both solutions.

All solutions were prepared by weight and ‘%’ always refers to weight %.

### SANS measurements

Static SANS measurements were carried out on LOQ at the ISIS facility (Rutherford Appleton Laboratory, Didcot, UK). LOQ uses incident wavelengths from 2.2 to 10.0 Å, sorted by time-of-flight, and a fixed sample-detector distance of 4.1 m. This provides access to scattering vectors  $q$  from 0.009 to 0.287 Å<sup>-1</sup>. The scattering intensity was

converted to the differential scattering cross-section in absolute units using the standard procedures at each facility.

Time-resolved SANS (TR-SANS) were performed on the D22 instrument at the Institut Laue Langevin (ILL, Grenoble, France). The wavelength  $\lambda$  was set at 6 Å, the peak flux of the cold source. The sample-to-detector distance was 4 m with a collimation at 5.6 m and a detector offset of 400 mm to maximize the available  $q$ -range ( $1.2 \times 10^{-2} \text{ Å}^{-1} < q < 0.26 \text{ Å}^{-1}$ ). A  $7 \times 10 \text{ mm}^2$  sample aperture was used, and the sample path length in the Biologic SFM-300 stopped-flow apparatus was 1 mm. Further experimental detail can be found in our previous publication.<sup>2</sup>

### Modelling of SANS data

Scattering curves from the Pluronic micelles with and without drug were fitted to a core-shell sphere (CSS) model combined with a hard-sphere structure factor using the SasView 3.0.0 software.<sup>20</sup> A Gaussian coil with  $R_g = 7 \text{ Å}$  was added to improve the modelling in the high- $q$  region, which originates from the PEO shell. From a combination of micellar size and solvent penetration (obtained from the fitted value of the scattering length density (sld) of the shell), it is possible to estimate an aggregation number,  $N_{agg}$ , as described in a previous publication.<sup>14</sup>

The scattering from Pluronic micelles with drug and varying amounts of DIMEB were fitted using a combined model comprising a core-shell sphere (CSS) interacting through a hard-sphere structure factor (for the micelles) and simple spheres (radius 10 Å) to model the cyclodextrins (no Gaussian coil was added in this case, in order to keep the number of parameters reasonably low). Polydispersity (with a Gaussian distribution of sizes) was applied to both the core and the shell.

### Fluorescence measurements

Measurements were performed on a Cary Eclipse fluorescence spectrophotometer (Varian, Oxford, UK).

Two regimes of drug concentration were used: dilute ( $10^{-3}$  wt%) and concentrated (2 wt%) for NP, PB and SAL and 0.3 % for LD, as determined by its aqueous solubility.<sup>21</sup>

The aqueous solutions were prepared using ultra-pure water (18.2 MΩ.cm).

The following excitation wavelengths were used for the drugs: Lidocaine:  $\lambda_{exc} = 262 \text{ nm}$ ; pentobarbital:  $\lambda_{exc} = 240 \text{ nm}$ ; naproxen sodium salt:  $\lambda_{exc} = 317 \text{ nm}$ ; sodium salicylate:  $\lambda_{exc} = 296 \text{ nm}$ .

The binding constant of the drugs to F127 micelles were determined using the method proposed by Almgren.<sup>22</sup>

$$\left( \frac{F_{\infty} - F_0}{F - F_0} \right) = \left( 1 + \frac{1}{K_{F127} C_M} \right) \quad \text{Eq. (1)}$$

where  $C_M$  is the micellized surfactant concentration with  $C_M = (C_S - \text{cmc})$ ,  $C_S$  being the total surfactant concentration,  $F$  is the measured fluorescence intensity,  $F_0$  and  $F_{\infty}$  are the fluorescence intensity when all the drug is free and complexed, respectively.  $K_{F127}$  is the binding constant of the drug to the micelle, obtained by fitting the experimental data.

$F_0$  is an experimental parameter, while  $F_{\infty}$  cannot always be obtained experimentally thus Eq. (1) is rearranged to obtain:

$$\left( \frac{F_0}{F - F_0} \right) = \left( \frac{F_0}{F_{\infty} - F_0} \right) \left( 1 + \frac{1}{K_{F127} C_M} \right) \quad \text{Eq. (2)}$$

Plots of  $F_0/(F-F_0)$  vs  $1/C_M$  give a linear plot, where the ratio of the y-intercept over the slope gives  $K_{F127}$ .

The binding constants of the drugs to F127 micelles were calculated using the cmc values presented in **Table 1** (obtained from UV-vis absorbance spectroscopy with methyl orange). The binding constant of each drug (in dilute conditions, at 10<sup>-3</sup>%) to cyclodextrin,  $K_{DIMEB}$ , was determined using the following expression:

$$F = \frac{(F_0 + F_{\infty} K_{DIMEB} [CD])}{1 + K_{DIMEB} [CD]} \quad \text{Eq. (3)}$$

where  $F$  is the measured fluorescence intensity,  $F_0$  and  $F_{\infty}$  are the fluorescence intensity when all the drug is free and complexed, respectively;  $F_0$  is the experimental value in all cases  $F_{\infty}$  is the experimental value for NP and SAL, whereas in the case of LD and PB,  $F_{\infty}$  value was obtained by fitting.  $[CD]$  is the concentration of free cyclodextrin, which, in these dilute systems, corresponds to the analytical concentration, since  $[CD] \gg [\text{drug}]$ . A non-linear least squares method was used to fit the experimental results to Eq (3) and obtain  $K_{DIMEB}$ . The  $[CD]$  concentration used was expressed in mass fraction (X) for consistency of units between all experiments; as a result, the binding constant, which is expressed in inverse of concentration units, X<sup>-1</sup>: g/g.



### **Cmc determination by UV-Vis absorbance**

The cmc of F127 micelles in the absence and presence of each drug was measured using methyl orange as a probe for UV-vis absorbance spectroscopy. Methyl orange is a dye with a strong absorbance in the visible region of the spectrum, sensitive to the nature of the microenvironment in which it is present. This probe was selected because it absorbs far from the drugs. A blue shift (lower wavelength) in the MO absorption maximum is observed when the probe is transferred from water to a less polar media.<sup>23</sup> Owing to this sensitivity, MO has been widely used for cmc determination.<sup>24</sup>

The absorption spectra of MO in the presence of increasing amounts of F127 were measured on a Jenway (Model 7315) uv-vis spectrophotometer in cells of 1 cm optical path length. The concentration of MO ( $4 \times 10^{-5}$  M) was kept constant. The position of the maximum is blue-shifted with increasing F127 concentration (**SI 1**) showing the transfer of MO from bulk water to the less polar micellar microenvironment, therefore signalling the onset of micellisation.

In general, the attribution of a single cmc value to this type of non-ionic surfactants is problematic;<sup>17</sup> indeed, a wide range of cmc values have been published for Pluronics, a fact generally attributed to batch-to-batch variation and the inherent polydispersity of the polymers, added to a dependence on the technique used. Extrapolation of straight lines can lead to important errors in the estimation of the cmc and we have opted for the fit of the absorbance maximum with a logistic curve, as this model accounts for aggregation processes, either cooperative or not.<sup>25</sup> In a “classical” surfactant, in which the transition is sharp, the cmc is associated with the inflection point. However, if aggregation occurs over a broad range of concentrations (as is the case), a criterion that better measures the onset of aggregation is preferred. We have considered here the cmc as the concentration at which 1% of the change in the trend of the fit occurs (which can be deduced easily from the logistic curve, **SI 2**).

### **NMR Measurements.**

Solutions of 5% F127 with 1 % drug salts or 0.65 % lidocaine in F127 and 0.3% in D<sub>2</sub>O. The <sup>1</sup>H 1D and 2D NMR spectra were recorded on a Bruker Avance 500 spectrometer operating at 500 MHz proton frequency. The (<sup>1</sup>H-<sup>1</sup>H) NOESY experiments were acquired with mixing time of 100, 300 and 500 ms; 512 experiments were performed in the F1 dimension with 16 scans for each of the t<sub>1</sub> increments and sweep width of 6.6 ppm. Selective <sup>1</sup>H-NOESY experiments were carried out by using

soft Gaussian pulses and library pulse sequence. Self-diffusion coefficients were measured by PFG experiments. A pulsed gradient unit capable of producing magnetic field pulse gradients in the z-direction of 53 G cm<sup>-1</sup> was used. All the experiments were performed using the bipolar pulse longitudinal eddy current delay (BPPLIED) pulse sequence. The duration of the magnetic field pulse gradients ( $\delta$ ) and the diffusion times ( $\Delta$ ) were optimized for each sample in order to obtain complete dephasing of the signals with the maximum gradient strength. In each DOSY experiment, a series of 64 spectra with 32K points were collected. For the investigated samples,  $\delta$  values were in the range 2-3 ms, while the  $\Delta$  values were in the range 0.1-0.5 s. The pulse gradients were incremented from 2 to 95% of the maximum gradient strength in a linear ramp. The temperature was set and controlled at 310K with an air flow of 535 l h<sup>-1</sup> in order to avoid any temperature fluctuations due to sample heating during the magnetic field pulse gradients.

Hydrodynamic radii of free and loaded F127 micelles in D<sub>2</sub>O, were calculated from the diffusion coefficients,  $D_0$ , using the Stokes- Einstein equation (Eq. 4), assuming that the aggregates are spherical and non-interacting.

$$R_h = \frac{k_B T}{6\pi\eta D_0} \quad \text{Eq. (4)}$$

where  $k_B$  is the Boltzman constant,  $T$  the absolute temperature and  $\eta$  the solvent viscosity. D<sub>2</sub>O viscosity was taken as 1.1×10<sup>-3</sup> Pa·s at 25° and extrapolated to 0.836×10<sup>-3</sup> Pa·s at 37°C from reference.<sup>26</sup>

### **Light scattering measurements**

Both size distributions and molecular weight determination of the micelles were obtained with a Malvern Zetasizer Nano light scattering apparatus with a laser wavelength of 633 nm. The samples were prepared in D<sub>2</sub>O (to match the conditions used for SANS) and filtered prior to the measurements by 0.22  $\mu$ m Millex syringe PVDF filters onto semi-micro glass cells, and the temperature fixed at 37.0 °C  $\pm$  0.1°C with the built-in Peltier in the cell compartment. The viscosities and refractive indices of D<sub>2</sub>O at 37°C were taken into account to obtain the particle size distribution from the analysis of the autocorrelation function, which was performed with the Zetasizer software. This built-in software uses cumulant and non-negative least squares

algorithms to calculate the size distribution; both methods have been used to analyse the DLS data and give consistent results. A  $dn/dc = 0.133 \text{ mL g}^{-1}$  was used for the molecular weight determination of the micelles. Considering the large range of surfactant concentration in the Debye plots (up to 5%), very good fits were achieved with a 2<sup>nd</sup> order polynomial (third virial coefficient in the  $c^2$  term).

Micellar aggregation numbers,  $N_{agg}$  (shown in **Table 2**) were calculated from the number of drug molecules inside the aggregates (**SI 3**), molecular weight of loaded and free F127 micelles (5%) at 37°C by using Eq. 5:

$$MW_{loaded\ micelle} = N_{agg} \times MW_{F127\ monomer} + N_{drug} \times MW_{drug} \quad \text{Eq. (5)}$$

## Results and Discussion

### Micellar structure: effect of the drugs, effect of cyclodextrin

#### *Effect of loading drugs in the micelles*

For the free and drug-loaded micelles at 37°C, the scattering length density (sld) of the core was fixed at  $0.4 \times 10^{-6} \text{ \AA}^{-2}$  (sld of PPO, corresponding to no solvent penetration). The sld of the shell was fitted and found to be ca.  $5.95 \times 10^{-6} \text{ \AA}^{-2}$ , reflecting a high level of hydration (92-95%) (**Table 3**). Neutrons are then mainly sensitive to the micellar core and the thickness of the hydrophilic shell cannot be determined in a very accurate way, within  $\pm 5 \text{ \AA}$ . For all micelles, the hard sphere volume fraction  $25 \pm 1\%$  and polydispersity was applied to the radius (0.15) and the shell (0.2). This model gives for 5% F127 micelles a core radius of  $45 \text{ \AA}$ , shell thickness of  $64 \text{ \AA}$  and  $N_{agg}$  of 40 (in good agreement with the value of 39 obtained for 3% F127 at 35°C using a different model).<sup>27</sup>

The scattering signal from micelles loaded with 0.5, 1 and 2% PB shows little variation from the free micelles (**Figure 1A**), with only a very slight decrease in intensity, reflecting a slight decrease in micellar size. In contrast, at 25°C, a slight increase in intensity had been observed (together with marginally stronger inter-micellar repulsion), which suggested a slight swelling of the micelles by the drug,<sup>1</sup> thus pointing to a shift in the balance of forces with temperature and compatible also with a small contribution of unspecific aggregates - typical of this type of block copolymers - which may still be present at this temperature. This slight decrease in size at 37°C is confirmed by

measurements of the hydrodynamic radius by DLS and the core radius in SANS (**Table 3**). The hydrodynamic radius of PB-loaded micelles obtained by diffusion NMR (16.6 and 7.5 nm) are higher and lower than the corresponding free micelles (9.0 nm and 8.8 nm) at 25 and 37°C, respectively, thus confirming the opposite effects (although minor) obtained at r.t. and physiological temperature.

In contrast, the presence of both naproxen and salicylate sodium salts produces a visible decrease in micellar size, as observed at 25°C,<sup>1</sup> which is more pronounced as the amount of drug increases, and is attributed to increased electrostatic repulsions inside the micelles, due to the partitioning of the charged drugs (**Figure 1B, Table 3**). At equivalent concentration, the addition of NP reduces the size of the micelles to a larger extent than SAL.

Finally, the addition of lidocaine induces a net increase in the scattered intensity and a net shift of the second oscillation (around ca.  $0.1 \text{ \AA}^{-1}$ ) to lower  $q$  values, reflecting a swelling of the micellar core (**Figure 1C, Table 3**). This unambiguously shows that the hydrophobic, uncharged drug becomes solubilized in the micellar core, as also observed at 25°C.<sup>1</sup> The sld of LD was not taken into account in the fits (equally for the other drugs) and  $\text{sld}_{\text{core}}$  was kept at  $0.4 \times 10^{-6} \text{ \AA}^{-2}$ . A two-shell model (with a core of LD) was attempted but did not improve the fits. This swelling of the micelles by lidocaine had previously been reported for concentrated solutions of F127 (18 %) with 1 and 2 % lidocaine, using a paracrystalline model to fit the data,<sup>7</sup> with an increase of mean radius from 43 Å with no lidocaine to 48 Å and 53 Å with 1 and 2% lidocaine, respectively.

Overall, the effect of the drugs on micellar size is similar to those previously observed at 25°C:<sup>1</sup> LD swells the micellar core, PB produces very minor changes, NP and SAL both shrink the micelles. This provides us with four different structures and scenarios to elucidate the competitive interactions in ternary systems formed by the same drugs with micelles and cyclodextrins.

#### *Disruptive effect of cyclodextrin; protective effect of drugs*

The addition of increasing amounts of dimethylated  $\beta$ -cyclodextrin (DIMEB) at 37°C produces a progressive rupture of the micelles, both for the free micelles and the drug-loaded micelles (**Figure 2**), as had been observed with this specific cyclodextrin at 25°C,<sup>1</sup> other Pluronics (P85 and P123)<sup>2</sup> and other PEO-PPO-based block-copolymers.<sup>14,</sup>

<sup>15</sup> Interestingly, the rupture of the drug-loaded micelles is hindered compared to the free micelles, i.e. higher amounts of DIMEB are required to produce a comparable reduction

in size, which is easily seen by observing overlapping scattering curves in **Figure 2**, or comparing micellar size obtained from fitting the curves to a core-shell model with a contribution from the cyclodextrins as spheres (**Table 4**), as described in the Experimental section. For instance, 11% of DIMEB need to be added to PB-loaded micelles to produce about the same effect as only 7% DIMEB on free micelles (**Figure 2A, Table 4**). Similarly, 13% DIMEB added to either PB- or NP-loaded micelles produces micelles with a comparable core-size than only 9% DIMEB added to free micelles (**Figure 2A, Table 4**). SAL-loaded micelles with 9% DIMEB are much larger than free micelles with the same amount of DIMEB (**Figure 2B, Table 4**), despite SAL-loaded micelles being smaller to start with (equally NP-loaded micelles). With LD, a protective effect had also been reported previously.<sup>7</sup> **Figure 2C** shows for instance that 7% DIMEB added to free F127 produces a scattering similar to 11% DIMEB added to LD-loaded micelles, or that 9% DIMEB added to free micelles yield a size similar to LD-loaded micelles with as much as 13% DIMEB added (**Table 4**). With LD however the comparison is less straightforward as LD-loaded micelles (in the absence of DIMEB) are larger than free F127 micelles.

Generally, drug-loaded micelles are more resistant to disruption against DIMEB than free F127 micelles, but how do each drug compare to the others?

If we compare the effect of NP and SAL, we observe that for the same amount of DIMEB (9 and 13%), micelles loaded with NP are larger than SAL-loaded micelles (**Figure 2B, Table 4**), despite NP-loaded micelles being slightly smaller to start with (**Figures 1B, Table 3**). In other words, NP is more efficient in protecting the micelles than SAL, despite the similarities in their chemical structure. Comparing LD and PB (**Figure 2C**), it appears that PB- and LD-loaded micelles with 11% added DIMEB show a very similar scattering (PB-loaded micelles marginally larger, **Table 4**); from these equivalent structures, an additional 2% DIMEB (up to 13% DIMEB) induces a larger extent of disruption in PB-loaded micelles (lower curve, **Figure 2C**) than in LD-loaded micelles, thus suggesting a higher protective effect of LD vs. PB (although the effect is quite moderate). Comparing PB and NP, it appears that for the same amount of added DIMEB (9 and 13%) the curves of PB- or NP-loaded micelles exactly overlap (**Figure 2A**), reflecting similar micelle sizes (**Table 4**); since PB-loaded micelles are larger to start with (**Table 3**), this suggests that NP has a higher protective effect. We note that NP, PB and SAL-loaded micelles have generally larger shell thicknesses, which may be

due to the superficial localization of these drugs (a point clarified later using 2D NMR), leading to higher hydration.

Overall, it appears that while all drugs protect the micelles against disruption by DIMEB, they do this to various extents. Over the range of compositions studied, we find that the protective effect is: NP>SAL, NP>PB and LD>PB. How do drugs ‘protect’ micelles against rupture by DIMEB? In these systems with three components, where each can interact with the two others, hindrance to micellar rupture may be attributed to either:<sup>1</sup> (1) a stabilization of the micelles by the drugs, controlled by drug-polymer interactions; (2) the formation of drug:cyclodextrin inclusion complexes, leading to a lower *effective* amount of cyclodextrin molecules available to rupture the micelles. Previous studies at 25°C<sup>1</sup> suggested that both mechanisms needed to be accounted for in the case of PB, while for NP and SAL competition alone (mechanism (2)) could be sufficient to explain the protective effect (the conditions at 25°C, however, did not allow us to exclude mechanism (1)). In order to elucidate the interactions present in these ternary systems, we next quantify the affinity of the molecules with each other, by measuring drug:CD binding constants (responsible for mechanism (2)) and the partitioning of the drugs within the micelles (responsible for mechanism (1)).

## Quantifying the drugs affinity to cyclodextrin and polymer

### *Drug:CD binding constants*

The binding constant of all four drugs to DIMEB was determined by fluorescence spectroscopy, using the natural fluorescence of the drugs. The addition of DIMEB to the drug solutions produces a hyperchromic effect, reflecting an interaction between the drugs and DIMEB. For all four drugs, a good fit of the plot of emission maxima vs. CD concentration is obtained by assuming a 1:1 stoichiometry (Eq. 3, **Figure 3A**). The values of the binding constants (**Table 5**) are lower than the ones determined at 25°C for all four drugs,<sup>1</sup> in agreement with an inclusion complex formation being an exothermic process.<sup>28-30</sup> Therefore, at 37°C, the competitive mechanism (2) - attributed to the drugs complexing with cyclodextrin - is weaker compared to the situation at 25°C.

The same measurements were carried out in the presence of Pluronic micelles (5%). In all cases, similar changes in the spectra were observed with the addition of cyclodextrin, clearly showing that drug:DIMEB complex formation still takes place in the presence of the polymer (**Figure 3B**). Therefore, in spite of drug partitioning within the micelles

and a lower drug:DIMEB binding (compared to 25°C), F127 and drug still compete for interacting with the cyclodextrins.

In order to quantitatively test mechanism (2), we consider an extreme scenario with no drug partitioning inside the micelles (i.e. all the drug interacts preferentially with DIMEB); this corresponds to the most competitive scenario between drug and polymer. Using the binding constants determined in **Table 5**, we have calculated the amount of free cyclodextrin,  $[CD]_{\text{free}}$ , (**SI 4**), i.e. the amount of *effective* cyclodextrin available to interact with the polymer for a *total* cyclodextrin concentrations,  $[CD]_{\text{tot}}$ , of 13% for 1% NP and PB and 9% for 1% SAL loaded micelles; in these conditions the loaded micelles present the same size than free micelles in the presence of  $[CD]_{\text{tot}}$  of 9 and 7% of DIMEB, respectively, as shown by SANS data (**Table 4**). The  $[CD]_{\text{free}}$  calculated (i.e. not complexed with the drug) would be 12.3% and 12.0% for PB and NP, respectively, for a  $[CD]_{\text{tot}}$  of 13%; and  $[CD]_{\text{free}} = 8\%$  for SAL at  $[CD]_{\text{tot}} = 9\%$  (these high values for uncomplexed CD are due to the relatively low drug:CD binding constants, cf **Table 5**, and the very high CD/drug ratio). Therefore, the amount of CD free to interact with the polymer is necessarily higher than the value of 9% (in the case of PB and NP) and 7% (for SAL), which induce a similar micellar size reduction in free micelles (**Table 4**). The *larger* amount of effective cyclodextrin (in the presence of the drugs) compared to the free micelles (empty aggregates) needed to induce the same extent of rupture, indicates that the loaded micelles are overall more stable against rupture. These results demonstrate that the presence of all the drugs protects the micelles against rupture by DIMEB (mechanism 1) and cannot be attributed exclusively to the binding of the drug to cyclodextrins (mechanism (2)). While the involvement of drug:polymer interactions (mechanism (1)) in protecting the micelles against DIMEB had already been established for PB at 25°C,<sup>1</sup> it was not shown for NP and SAL at that lower temperature. Instead, here at 37°C we are able to show the important role of this mechanism in the protective effect of all the model drugs studied. Therefore, in the next section we measure the partitioning of the drugs within F127 micelles.

#### *Binding of drugs to F127 micelles*

The binding constant of the drugs to F127 micelles was measured at two drug concentrations ( $10^{-3}$  and 2%). The addition of F127 produces different changes in the drugs emission spectra, which are dependent on the drug and its concentration. In the case of NP and SAL, no change is observed at low drug concentration, while a

hyperchromic effect without spectral shift is observed at high drug concentration. This behaviour is the same as observed with the addition of DIMEB (previous section) and shows that no partitioning occurs at low NP or SAL concentration, and is not easily detected even at high concentration of SAL. Instead, in the case of LD, an increase in the emission intensity is observed at both drug concentrations studied ( $10^{-3}$  and 0.3%), confirming that partitioning takes place in both dilute and concentrated conditions. In addition, at 0.3% LD, a clear red shift in the emission band centered at 290 nm is observed (**SI 5A**), as observed when the polarity of the surroundings decreases,<sup>1</sup> thus showing the transfer of LD from water to a less polar environment inside the aggregates. In the case of PB, an increase in the emission intensity is obtained - thus reflecting an interaction with F127 micelles – but no spectral shift (**SI 5B**). Considering the dependence of the position of the emission maximum on solvent polarity,<sup>1</sup> this observation suggests that PB does not experience a large change in polarity when interacting with F127 micelles. These findings thus support a localization of LD deep inside the aggregates (in a non-polar region) and a localization of PB on the surface of the micelles, in close contact with the bulk water, which would thus explain the very limited structural changes to the micelles when loaded with PB (**Figure 1A, Table 3**). These considerations on drug localization are further discussed with results from 2D NMR (next section).

Fitting the experimental data to Eq. 2 (**Table 6, Figure 4**) shows that increasing drug concentration produces an important increase in partitioning within the micelles. The dependence of partitioning on solubilize concentration has been reported previously,<sup>31, 32</sup> but not widely studied and therefore is not well understood. Comparing the binding constants of these drugs to F127 at 37°C with those previously obtained at 25°C (shown in **Table 6**) also shows a strong increase with temperature. From a practical point of view, this is a very interesting result because the increase in partition increases the stability of the drug-micelle complex against dilution.<sup>32</sup> In addition, a higher partition implies that a larger amount of drug molecules are present within the micellar phase than at lower temperature, hence their contribution to the stabilisation of the micelles should be higher, in good agreement with the important role of mechanism (1) at this temperature, pointed out for all the drugs, and not observed, but probably also important, at 25°C. The increase in partition with temperature has been reported previously for other drugs<sup>33</sup> and dyes.<sup>18</sup> However, the increase of PB partition, in particular, is quite striking (more than 100 times higher than at 25°C).



Overall, the trend in micellar partitioning, at both drug concentrations, is: PB > LD > NP > SAL. This result differs from that observed at 25°C where LD presented the highest partitioning.<sup>1</sup> In octanol/water mixtures, the log P ( $= [\text{solute}]_{\text{octanol}}/[\text{solute}]_{\text{neutral, H}_2\text{O}}$ ) is defined to quantify the partition of neutral compounds. In ionisable molecules, partitioning depends on pH, hence a new parameter is defined to take into account the ionization process:  $\log D = \log [\text{solute}]_{\text{octanol}}/([\text{solute}]_{\text{neutral, H}_2\text{O}} + [\text{solute}]_{\text{ionized, H}_2\text{O}})$ . The partitioning values at the measured natural pH of F127/drug solutions was estimated from a range of values provided at different pH,<sup>34</sup> resulting in the following trend: SAL (-1.36) < NP (0.32) < PB (1.0) < LD (2.3). Clearly, salicylate has no tendency to partition in apolar octanol; this explains the difficulty in obtaining a measure of the binding to F127 (at low concentration) and the very low partition determined (at high concentration) (**Table 6**). The trend in Log D is in very good agreement with our results, except for PB that was found to partition much better than molecular LD.

Partition in the micelles, however, does not seem to correlate with the protective effect of the drugs on the micelles; this is clearly demonstrated by PB behaviour, which presents the highest partitioning, but produces small changes in the size of the micelle, and is less effective than LD or NP in preventing the rupture of the micelles by DIMEB. The main difference of PB, compared to the other drugs, seems to be its surface localisation in the micelles (suggested by fluorescence spectroscopy). The specific localisation of a drug within a micelle is determined by the hydrophilic-hydrophobic balance of the drug and its specific structure, and this solubilisation locus, in turn, impacts drug loading.<sup>35</sup> Therefore, a different localisation of PB – in a region matching its polarity - may explain its peculiar properties (i.e. high partitioning, striking increase in partitioning with temperature, low impact on micellar structure) and a lower protective effect against micellar disruption.

Therefore, the localisation of the various drugs – more than the value of their partitioning - may be an important factor to consider.

In order to examine this important parameter, we next use NOESY NMR to probe drug localization within the polymeric aggregates.

### **Localisation of the drugs within the aggregates**

For all four drugs studied, <sup>1</sup>H high-resolution spectra were obtained in pure D<sub>2</sub>O solution as well as in the presence of F127. No chemical shift or other spectral changes

of the drugs were observed by adding the polymer, confirming that no conformational changes are induced by the polymer.

Useful information for the assessment of drug- polymer interactions can be obtained by 2D NMR  $^1\text{H}$ - $^1\text{H}$  correlation spectroscopy based on the nuclear Overhauser enhancement (NOE). The fundamental theory and main applications to this type of systems have been reported in reference<sup>16</sup> and are not repeated here. In the remaining of this section, F127 spectral features are mentioned as a singlet at 1.13 ppm, assigned to the PPO methyl group, and a multiplet in the 3.68-3.42 ppm range, assigned to the PEO blocks. The proton spectra of the drugs are reported in Supporting information (**SI 6-9**).

The NOESY spectrum of PB in Pluronic F127/D<sub>2</sub>O solution (**SI 10**) shows a strong overlap of the CH<sub>2</sub> protons with PPO methyl group, thus severely limiting the possibility of using PPO methyl group as a probe for interaction. Nevertheless, the PEO signal (although affected by T1 noise) gives detectable cross peaks with PB, revealing an interaction between the polymer PEO protons with the three methyl groups of PB. This suggests a very superficial localisation of PB (or at least its apolar alkyl tail) within the micelles (**Scheme 2**), in very good agreement with previous fluorescence results<sup>1</sup> and the very limited changes in micellar structure upon drug partitioning (**Figure 1A**).

$^1\text{H}$ - $^1\text{H}$  NOESY measurements of NP and F127 (**SI 11**) mixture reveal NOE cross peaks between the aromatic part of the molecule and the CH<sub>3</sub> of PPO, indicating a close spatial relationship of the drug with the PPO blocks of the polymer. Unfortunately, the PEO signal is too strong and affected by T1 noise, thus it is not possible to assess whether it gives NOE with other protons. Despite this technical limitation, this result is in any case consistent with the aromatic part of NP interacting with the micellar core. Based on naproxen structure, having a hydrophobic naphthalene ring but a negative charge, a localisation at the core/shell interface is expected (**Scheme 2**).

For salicylate, both 2D NOESY and ROESY experiments show an absence of cross peaks between the polymer and the drug molecule (**SI 12**). Similarly, no changes in the  $^1\text{H}$ -NMR spectrum are detectable. These results show that SAL does not interact either with the micellar core or corona. Our partitioning data (**Table 6**) show a very limited partitioning of SAL within the micelles, reflecting a very low affinity for the polymer, despite the presence of an aromatic ring. A very low number of molecules partitioning could explain the impossibility of detecting cross-peaks with NMR. Indeed, at acidic pH (pH 1), where SAL becomes uncharged, strong NOE are detected, showing a localisation similar to NP (**SI 13**), and demonstrating the strong effect of charge on

partitioning. Recent studies by fluorescence (using C153 as a corona hydration probe)<sup>36</sup> suggest that both salicylic and salicylate ion reside in the corona region of Pluronic P85. Our combined results indicate that SAL in its ionized form is not inside the micelle, in spite of its interaction with the micelle (pointed out by changes in fluorescence and micellar structure by SANS), thus it is more likely to be adsorbed onto the micellar surface.

Finally, with lidocaine, a severe overlap of drug and polymer signals hamper the interpretation of NOE data, as the signal from the CH<sub>3</sub> protons of LD overlap with the methyl groups of PPO (**SI 14**). However, it is possible to establish that the aromatic protons of lidocaine do not show cross peaks with the PEO signals, thus reflecting a very limited interaction with the corona and supporting a deeper localisation of LD within the micelles, as also suggested by fluorescence (less polar microenvironment) and shown by SANS data (swelling of the core region).

Overall, NMR data confirm that all drugs partition into different locations within the aggregates (**Scheme 2**), with LD partitioning close to the core, NP at the core/corona interface and PB near the surface. The solubilisation locus of SAL could not be determined, likely due to its very limited partitioning, but all results taken together suggest a more superficial localization than NP. With this knowledge, and to further examine the specific role of the localisation of these very different drugs on the stability of the micelles, we next measure their impact on F127 critical micellar concentration.

### **Critical micelle concentration**

The cmc value of F127, alone and in the presence of each of the four drugs (**SI 2**), was determined in water using the method described in the experimental section (**SI 1**).

The cmc value of F127 at 25°C is  $1.4 \pm 0.13\%$  (**Table 1**). This value is lower but in good agreement with the one obtained by Desai et al.<sup>37</sup> by surface tension (2.0%) and ethyl orange spectral shift (2.5%), but higher than the value of 0.26% (0.20 mmol/dm<sup>3</sup>) obtained by Sharma et al. by SANS<sup>9</sup> or 0.12% (w/v) obtained by surface tension measurements<sup>38</sup> or by isothermal titration microcalorimetry (0.197 mM or 0.25% at 28°C).<sup>39</sup>

The same spectral changes in the presence of the drugs were observed, namely, a blue shift of the absorption maximum. The presence of the drugs without F127 does not produce any change in the MO spectrum. Therefore, the changes observed correspond to the interaction of MO with F127.

The presence of LD produces a decrease in the cmc at 25°C, in good agreement with the increase in micellar size observed by SANS. The addition of PB also leads to a decrease in the cmc to  $0.9\pm0.3\%$  (at 25°C), showing that the presence of PB does affect the micellization ability of the polymer, despite SANS showing very little change in the size of the aggregates.<sup>1</sup> Therefore, a stabilization of the micelles (lowering of the cmc) could explain the protective effect of both PB and LD against DIMEB at that temperature.<sup>1</sup> In fact, our previous study at 25°C had shown that the protective effect of PB could not be attributed to mechanism (2) alone.<sup>1</sup> In contrast, the presence of both NP and SAL at 25°C slightly increases the cmc of F127 (**Table 1**), in good agreement with the binding of charged species to the polymer chains inducing an increase in solubility, as described elsewhere for anions.<sup>40</sup>

The increase in temperature produces a marked decrease in the cmc value of free micelles, as previously observed.<sup>39, 41</sup> The same effect is observed in drug-loaded micelles. Solubilisation of LD inside the micellar core decreases the cmc at 37°C, while it is increased with the other drugs: only slightly for PB and quite substantially for both NP and SAL. Interestingly, the cmc measurements at 25°C and 37°C confirm the contrasting effect PB has on the micellar structure at these two temperatures, shown by SANS and confirmed by diffusion NMR (**Figure 1A** and reference).<sup>1</sup>

The free energy of the monomers inside the loaded aggregates is given by  $\Delta G^0 = RT \ln \text{cmc}$ , showing clearly that at higher temperatures the free micelles are more stable against disruption by DIMEB. The presence of LD further stabilizes the micelles against disruption, while at 37°C the other drugs (PB, NP, SAL) do not stabilize energetically the aggregates (as inferred from the higher cmc values) and the presence of these drugs is therefore unlikely to act as a preventive mechanism against micelle disruption. Moreover, the cmc of the NP-loaded micelles is higher than the free and PB-loaded micelles; its partition is also lower than PB (**Table 6**), but overall its protective effect is stronger (**Figure 2A**, **Table 4**).

Since neither the cmc nor the extent of partitioning seem to directly correlate with the protective effect of the drugs against DIMEB, maybe the amount of drug molecules present inside the aggregates – which take into account both partitioning and micellar size – could explain the effects observed. For this purpose, we next used static light scattering (SLS) to determine the molecular weight of the micelles in the absence and presence of the drugs.

### Number of drug molecules per micelle and $N_{agg}$ (DLS and SLS)

To gain further insight on the micellization of F127 in the presence of drugs and compare to the SANS data, the dimensions and molar mass of the micelles were obtained by DLS and SLS in D<sub>2</sub>O at 37°C (**Table 2**). In agreement with SANS, micellar size is reduced slightly with drug loading (**Table 3**). With LD, the change is minor, but SANS had shown that the core was swollen by penetration of the drug (a difference in shell thickness – outside the detection limit of SANS – could explain the similar hydrodynamic size measured by DLS). The diffusion coefficients of NP and SAL-loaded micelles as a function of concentration lie well above those of the free micelles, and PB and LD-loaded micelles (**SI 15**). The diffusion coefficients at infinite dilution are: 25.9 (F127), 26.4 (LD), 29.2 (PB), 31.2 (SAL) and 33.3  $\mu\text{m}^2\text{s}^{-1}$  (NP), indicating unambiguously that free micelles diffuse more slowly than drug-loaded ones. The molecular weight of the micelles, determined by SLS, is also affected by the presence of the drugs (**Table 2**), as reported with P103 in the presence of flurbiprofen.<sup>42</sup> Combining the values of the cmc (**Table 1**), MW of the loaded micelles (**Table 2**) and drug:F127 binding constants (**Table 6**), and neglecting changes in partition with drug concentration, the number of drug molecules inside the micelles can be estimated (**Table 2**, **SI 3**). These results show that the number of drug molecules within the aggregates do not hold the key for the protective effect, for instance with a lower amount of NP being more efficient than a higher amount of PB or SAL molecules.

### Time-resolved SANS

SANS measurements combined with a stopped-flow set-up add further insight into the role of drugs in hindering cyclodextrins-triggered disruption of micelles (**Figure 5**). These measurements were performed at 25°C and a slightly lower concentration of F127 (4%). When adding 5% DIMEB to Pluronic micelles loaded with 1% PB or NP, the break-up of the micelles is gradual: while there is a very fast drop in intensity after 100 ms (second curve), which reflects an extensive break-up of the micelles, the next steps (to the final equilibrium structure) take 100s of seconds. This is in stark contrast to the free micelles, where the break-up was shown to be instantaneous (ca ~ 100 ms, the detection limit of the technique), namely: from the first frame at 100 ms, all curves superimposed perfectly.<sup>2</sup> This result shows that the presence of drugs not only affects the equilibrium structure (more DIMEB is needed to achieve the same extent of rupture) but also seem to affect the kinetic pathways of the process.

As discussed above, the protective effect is not directly related to partitioning, neither to the number of drug molecules inside the aggregates. The slower kinetics point to processes taking place within the micelles, which could indeed be mediated by the precise localisation of the drugs within the aggregates. How can the locus of solubilisation determine the protective effect of these drugs against DIMEB? Previous results have shown that the methyl groups in position 3 of DIMEB interact with the methyl PPO groups of the micellar core, and that this interaction may be responsible for the break-up of F127 micelles.<sup>16</sup> NP is located at the core/corona interface, so its presence could directly prevent the contact of DIMEB with the PPO core. PB is located far from the PPO methyl groups and nearer to the PEO corona, which is unlikely to be directly involved in the rupture by DIMEB, but PB could act by hindering the diffusion of CD to the micellar core from the micelle surface. Binding of the drugs to DIMEB *within* the aggregates may also be key to the protective effect.

The formation/dissociation of drug/cyclodextrin inclusion complex have a lifetime in the range of milliseconds,<sup>30</sup> while the exit of common arenes molecules from micelles takes around 10 ms.<sup>43</sup> Overall, the timings revealed by TR-SANS demonstrate that it is not the snatching of the drugs from aqueous DIMEB nor inclusion complex formation in the aqueous pool which produce a delay time in breaking the micelles. Instead, the origin of drug protection seems to lie with events happening inside the aggregates, possibly involving the co-aggregation of these complexes within the aggregates, as has been observed elsewhere.<sup>44-46</sup>

## Conclusion

In this work, we have studied the effect of four drugs of varying structures in reducing the extent of Pluronic F127 demicellisation, which is triggered by dimethylated  $\beta$ -cyclodextrin (DIMEB). Using a wide combination of techniques, we have examined two possible mechanisms of protection: (1) a stabilization of the micelles by the drugs, controlled by drug-polymer interactions; (2) the role of drug:cyclodextrin inclusion complex formation (which leads to a lower *effective* amount of cyclodextrin molecules available to rupture the micelles). The large variation in drug structure and properties enables us to examine, one after the other, various factors that underlie these two mechanisms and could be responsible for micelle protection.

Our results show that the presence of these drugs in the aggregates impacts the size and structure of the loaded micelles in different ways (SANS data): while PB has a very small impact on micellar structure, SAL and NP reduce micellar size through intra-micellar electrostatic repulsions, and LD swells the micellar core. We were able to relate these outcomes to drug structure and their solubilisation locus within the aggregates, for the first time measured by 2D NOESY NMR: PB has a very superficial localisation at the micellar surface, while NP is located at the core/corona interface; SAL localisation could not be detected (due to very low partitioning), but adopts a similar locus than NP at acidic pH; LD is localised in a non-polar environment, which concurs with its partitioning within the hydrophobic core.

High temperature (37°C) promotes the partitioning of all the drugs, while decreasing their binding to DIMEB. This shift in the balance of forces (compared to 25°C)<sup>1</sup> enables us to establish that, at this temperature, the mechanism of protection is not due to a competitive complexation of the drugs with DIMEB (mechanism (2)); instead, it is the presence of the drugs within the aggregates which itself is responsible for the protective effect. However, cmc measurements show that the drugs do not increase the free energy of the monomers inside the aggregates (apart from LD) hence their impact on aggregation is not a protective factor in itself.

Time-resolved SANS in the presence of drug-loaded aggregates reveal that the presence of drugs considerably slows down the process of rupture (to 100s of seconds), compared to the free micelles (< 100 ms).<sup>2</sup>

Overall, our results show that neither partitioning, drug:CD binding, or the decrease in cmc hold the key to the protective effect of the drugs and their differences. It is suggested instead that processes taking place within the aggregates, thus modulated by the localisation of the drugs, impact micellar rupture. In particular, the co-aggregation of drug:CD inclusion complexes, or hindrance due to physical contact between DIMEB and the methyl groups of PPO, as previously suggested,<sup>16</sup> may be responsible for this protective effect.

On the whole, this work provides new insights into cyclodextrin-induced demicellisation, the importance of drug solubilisation locus within polymeric micelles, and inclusion complex formation between drugs and cyclodextrins, which are highly relevant to the controlled delivery of active compounds from polymeric micelles or cyclodextrins, but also offer a fundamental understanding into competitive molecular

processes that control interactions and thus equilibrium structures in multi-component systems.

### Supporting Information

UV-Vis absorbance spectra of Methyl Orange (MO); calculations of the amount of free DIMEB and number of drugs inside F127 micelles; fluorescence emission spectra of drug-loaded micelles; NMR spectra; determination of the cmc from MO absorbance spectra; diffusion coefficient of the micelles obtained from DLS. This material is available free of charge at <http://pubs.acs.org>.

### References

1. Valero, M.; Dreiss, C. A., Growth, Shrinking, and Breaking of Pluronic Micelles in the Presence of Drugs and/or  $\beta$ -Cyclodextrin, a Study by Small-Angle Neutron Scattering and Fluorescence Spectroscopy. *Langmuir* **2010**, 26, (13), 10561-10571.
2. Valero, M.; Grillo, I.; Dreiss, C. A., Rupture of Pluronic Micelles by Di-Methylated  $\beta$ -Cyclodextrin Is Not Due to Polypseudorotaxane Formation. *The Journal of Physical Chemistry B* **2012**, 116, (4), 1273-1281.
3. Alvarez-Lorenzo, C.; Sosnik, A.; Concheiro, A., PEO-PPO Block Copolymers for Passive Micellar Targeting and Overcoming Multidrug Resistance in Cancer Therapy. *Curr. Drug Targets* **2011**, 12, (8), 1112-1130.
4. Duncan, R.; Vicent, M. J., Polymer therapeutics-prospects for 21st century: The end of the beginning. *Adv. Drug Del. Rev.* **2013**, 65, (1), 60-70.
5. Alakhova, D. Y.; Kabanov, A. V., Pluronics and MDR Reversal: An Update. *Mol. Pharm.* **2014**, 11, (8), 2566-2578.
6. Valle, J. W.; Armstrong, A.; Newman, C.; Alakhov, V.; Pietrzynski, G.; Brewer, J.; Campbell, S.; Corrie, P.; Rowinsky, E. K.; Ranson, M., A phase 2 study of SP1049C, doxorubicin in P-glycoprotein-targeting pluronics, in patients with advanced adenocarcinoma of the esophagus and gastroesophageal junction. *Invest. New Drugs* **2010**, 29, (5), 1029-1037.
7. Dreiss, C. A.; Nwabunwanne, E.; Liu, R.; Brooks, N. J., Assembling and de-assembling micelles: competitive interactions of cyclodextrins and drugs with Pluronics. *Soft Matter* **2009**, 5, (9), 1888-1896.
8. Sharma, P. K.; Reilly, M. J.; Jones, D. N.; Robinson, P. M.; Bhatia, S. R., The effect of pharmaceuticals on the nanoscale structure of PEO-PPO-PEO micelles. *Colloids Surf. B. Biointerfaces* **2008**, 61, (1), 53-60.
9. Sharma, P. K.; Bhatia, S. R., Effect of anti-inflammatories on Pluronic® F127: micellar assembly, gelation and partitioning. *Int. J. Pharm.* **2004**, 278, (2), 361-377.
10. Nagarajan, R.; Barry, M.; Ruckenstein, E., Unusual selectivity in solubilization by block copolymer micelles. *Langmuir* **1986**, 2, (2), 210-215.
11. Davis, M. E.; Brewster, M. E., Cyclodextrin-based pharmaceuticals: past, present and future. *Nat. Rev. Drug Discov.* **2004**, 3, (12), 1023-1035.
12. Kang, Y.; Guo, K.; Li, B.-J.; Zhang, S., Nanoassemblies driven by cyclodextrin-based inclusion complexation. *Chem. Commun.* **2014**, 50, (76), 11083-11092.



13. Jiang, L.; Yan, Y.; Huang, J., Versatility of cyclodextrins in self-assembly systems of amphiphiles. *Adv. Colloid Interface Sci.* **2011**, 169, (1), 13-25.
14. González-Gaitano, G.; Müller, C.; Radulescu, A.; Dreiss, C. A., Modulating the Self-Assembly of Amphiphilic X-Shaped Block Copolymers with Cyclodextrins: Structure and Mechanisms. *Langmuir* **2015**, 31, (14), 4096-4105.
15. González-Gaitano, G.; da Silva, M. A.; Radulescu, A.; Dreiss, C. A., Selective Tuning of the Self-Assembly and Gelation of a Hydrophilic Poloxamine by Cyclodextrins. *Langmuir* **2015**, 31, (20), 5645-5655.
16. Castiglione, F.; Valero, M.; Dreiss, C. A.; Mele, A., Selective Interaction of 2,6-Di-O-methyl- $\beta$ -cyclodextrin and Pluronic F127 Micelles Leading to Micellar Rupture: A Nuclear Magnetic Resonance Study. *The Journal of Physical Chemistry B* **2011**, 115, (29), 9005-9013.
17. Kabanov, A. V.; Nazarova, I. R.; Astafieva, I. V.; Batrakova, E. V.; Alakhov, V. Y.; Yaroslavov, A. A.; Kabanov, V. A., Micelle Formation and Solubilization of Fluorescent Probes in Poly(oxyethylene-b-oxypropylene-b-oxyethylene) Solutions. *Macromolecules* **1995**, 28, (7), 2303-2314.
18. Perry, C. C.; Sabir, T. S.; Livingston, W. J.; Milligan, J. R.; Chen, Q.; Maskiewicz, V.; Boskovic, D. S., Fluorescence of commercial Pluronic F127 samples: Temperature-dependent micellization. *J. Colloid Interface Sci.* **2011**, 354, (2), 662-669.
19. Bhat, P. A.; Rather, G. M.; Dar, A. A., Effect of Surfactant Mixing on Partitioning of Model Hydrophobic Drug, Naproxen, between Aqueous and Micellar Phases. *The Journal of Physical Chemistry B* **2009**, 113, (4), 997-1006.
20. DMR-0520547, D. p. u. N. a. Sasview. [www.sasview.org](http://www.sasview.org) (01/jan/2015),
21. Kang, L.; Jun, H. W.; McCall, J. W., Physicochemical studies of lidocaine-menthol binary systems for enhanced membrane transport. *Int. J. Pharm.* **2000**, 206, (1-2), 35-42.
22. Almgren, M.; Grieser, F.; Thomas, J. K., Dynamic and static aspects of solubilization of neutral arenes in ionic micellar solutions. *J. Am. Chem. Soc.* **1979**, 101, (2), 279-291.
23. Reeves, R. L.; Kaiser, R. S.; Maggio, M. S.; Sylvestre, E. A.; Lawton, W. H., Analysis of the Visual Spectrum of Methyl Orange in Solvents and in Hydrophobic Binding Sites. *Can. J. Chem.* **1973**, 51, (4), 628-635.
24. Lin, Y.; Alexandridis, P., Cosolvent Effects on the Micellization of an Amphiphilic Siloxane Graft Copolymer in Aqueous Solutions. *Langmuir* **2002**, 18, (11), 4220-4231.
25. Aguiar, J.; Carpena, P.; Molina-Bolívar, J. A.; Carnero Ruiz, C., On the determination of the critical micelle concentration by the pyrene 1:3 ratio method. *J. Colloid Interface Sci.* **2003**, 258, (1), 116-122.
26. Cho, C. H.; Urquidi, J.; Singh, S.; Robinson, G. W., Thermal Offset Viscosities of Liquid H<sub>2</sub>O, D<sub>2</sub>O, and T<sub>2</sub>O. *The Journal of Physical Chemistry B* **1999**, 103, (11), 1991-1994.
27. Joseph, J.; Dreiss, C. A.; Cosgrove, T.; Pedersen, J. S., Rupturing Polymeric Micelles with Cyclodextrins. *Langmuir* **2007**, 23, (2), 460-466.
28. Inoue, Y.; Hakushi, T.; Liu, Y.; Tong, L.; Shen, B.; Jin, D., Thermodynamics of molecular recognition by cyclodextrins. 1. Calorimetric titration of inclusion complexation of naphthalenesulfonates with .alpha.-, .beta.-, and .gamma.-cyclodextrins: enthalpy-entropy compensation. *J. Am. Chem. Soc.* **1993**, 115, (2), 475-481.
29. Loftsson, T.; Brewster, M. E., Pharmaceutical Applications of Cyclodextrins. 1. Drug Solubilization and Stabilization. *J. Pharm. Sci.* **1996**, 85, (10), 1017-1025.

30. Stella, V. J.; Rao, V. M.; Zannou, E. A.; Zia, V., Mechanisms of drug release from cyclodextrin complexes. *Adv. Drug Del. Rev.* **1999**, 36, (1), 3-16.
31. Gadelle, F.; Koros, W. J.; Schechter, R. S., Solubilization of Aromatic Solutes in Block Copolymers. *Macromolecules* **1995**, 28, (14), 4883-4892.
32. Choucair, A.; Eisenberg, A., Interfacial Solubilization of Model Amphiphilic Molecules in Block Copolymer Micelles. *J. Am. Chem. Soc.* **2003**, 125, (39), 11993-12000.
33. Kadam, Y.; Yerramilli, U.; Bahadur, A.; Bahadur, P., Micelles from PEO–PPO–PEO block copolymers as nanocontainers for solubilization of a poorly water soluble drug hydrochlorothiazide. *Colloids Surf. B. Biointerfaces* **2011**, 83, (1), 49-57.
34. ChemAxon Chemicalize.org. [www.chemicalize.org](http://www.chemicalize.org) (02/june/2014),
35. Torchilin, V. P., Structure and design of polymeric surfactant-based drug delivery systems. *J. Controlled Release* **2001**, 73, (2–3), 137-172.
36. Parekh, P.; Ganguly, R.; Aswal, V. K.; Bahadur, P., Room temperature sphere-to-rod growth of Pluronic<sup>®</sup> P85 micelles induced by salicylic acid. *Soft Matter* **2012**, 8, (21), 5864-5872.
37. Desai, P. R.; Jain, N. J.; Sharma, R. K.; Bahadur, P., Effect of additives on the micellization of PEO/PPO/PEO block copolymer F127 in aqueous solution. *Colloids Surf. Physicochem. Eng. Aspects* **2001**, 178, (1–3), 57-69.
38. Wanka, G.; Hoffmann, H.; Ulbricht, W., Phase Diagrams and Aggregation Behavior of Poly(oxyethylene)-Poly(oxypropylene)-Poly(oxyethylene) Triblock Copolymers in Aqueous Solutions. *Macromolecules* **1994**, 27, (15), 4145-4159.
39. Bouchemal, K.; Agnely, F.; Koffi, A.; Ponchel, G., A concise analysis of the effect of temperature and propanediol-1, 2 on Pluronic F127 micellization using isothermal titration microcalorimetry. *J. Colloid Interface Sci.* **2009**, 338, (1), 169-176.
40. Deyerle, B. A.; Zhang, Y., Effects of Hofmeister Anions on the Aggregation Behavior of PEO–PPO–PEO Triblock Copolymers. *Langmuir* **2011**, 27, (15), 9203-9210.
41. Bakshi, M. S.; Sachar, S., Influence of temperature on the mixed micelles of Pluronic F127 and P103 with dimethylene-bis-(dodecyldimethylammonium bromide). *J. Colloid Interface Sci.* **2006**, 296, (1), 309-315.
42. Alexander, S.; Cosgrove, T.; Castle, T. C.; Grillo, I.; Prescott, S. W., Effect of Temperature, Cosolvent, and Added Drug on Pluronic–Flurbiprofen Micellization. *The Journal of Physical Chemistry B* **2012**, 116, (37), 11545-11551.
43. Mittal, K. L.; Fendler, E. J., *Solution behaviour of surfactants: Theoretical and applied aspects. Vol. 1.* Plenum press: New York, 1982; Vol. 1.
44. Messner, M.; Kurkov, S. V.; Jansook, P.; Loftsson, T., Self-assembled cyclodextrin aggregates and nanoparticles. *Int. J. Pharm.* **2010**, 387, (1–2), 199-208.
45. Tsianou, M.; Fajalia, A. I., Cyclodextrins and Surfactants in Aqueous Solution above the Critical Micelle Concentration: Where Are the Cyclodextrins Located? *Langmuir* **2014**, 30, (46), 13754-13764.
46. da Silva, M. A.; Weinzaepfel, E.; Afifi, H.; Eriksson, J.; Grillo, I.; Valero, M.; Dreiss, C. A., Tuning the Viscoelasticity of Nonionic Wormlike Micelles with  $\beta$ -Cyclodextrin Derivatives: A Highly Discriminative Process. *Langmuir* **2013**, 29, (25), 7697-7708.

**Table 1.** Critical micellar concentration (cmc) of F127 micelles, free and loaded with 1% drug (0.3 wt% for lidocaine), at 25°C and 37°C.

System	cmc / wt% (298 K)	cmc / wt% (310K)
<b>F127</b>	1.4 ± 0.13	0.42 ± 0.013
<b>LD:F127</b>	0.38 ± 0.12	0.174 ± 0.009
<b>PB:F127</b>	0.9 ± 0.3	0.65 ± 0.09
<b>NP:F127</b>	5 ± 2	1.7 ± 0.5
<b>SAL:F127</b>	5 ± 1	0.8 ± 0.1

**Table 2.** Molecular mass, number of drug molecules inside the aggregates and aggregation number of F127 micelles in D<sub>2</sub>O at 37°C, in the presence of 1% drug (0.67% LD) determined by SLS and SANS.

SYSTEM	MW/kDa	N <sub>drug</sub>	N <sub>agg</sub>	N <sub>agg</sub> /SANS
<b>F127</b>	419	-	33	39
<b>Lidocaine</b>	322	74 ± 23	24	56
<b>Pentobarbital</b>	323	293 ± 24	20	37
<b>Naproxen</b>	234	168 ± 22	15	26
<b>Salicylate</b>	370	240 ± 30	26	30

**Table 3.** Structural parameters obtained from DLS ( $R_H$ ) and SANS for the free and drug-loaded F127 micelles (5%) in D<sub>2</sub>O at 37°C. SANS data were fitted to a core-shell form factor interacting through a hard-sphere structure factor; a Gaussian coil ( $R_g = 7 \text{ Å}$ ) was used to describe the contribution in the high- $q$  region (cf. Experimental section).

	$R_H$ /nm DLS <sup>b</sup>	Core Radius /Å	Shell Thickness /Å	Shell sld /Å <sup>-2</sup>	Solvent penetration in shell /%	$N_{agg}$	Total radius /nm
<b>No drug</b>	10.9 <sup>b</sup> (3.1)	45	64	$5.89 \times 10^{-6}$	92	40	10.9
<b>LD 0.67%</b>	10.9 (1.8)	51	66	$5.91 \times 10^{-6}$	92	56	11.7
<b>PB 1%</b>	10.5 (2.0)	43	70	$5.94 \times 10^{-6}$	92	37	11.3
<b>PB 2%</b>	-	43	68	$5.96 \times 10^{-6}$	93	35	11.1
<b>NP 1%</b>	10.1 (2.4)	39	63	$5.97 \times 10^{-6}$	93	26	10.2
<b>NP 2%</b>	-	38	58	$6.07 \times 10^{-6}$	95	23	9.6
<b>SAL 1%</b>	10.3 (1.6)	41	64	$5.94 \times 10^{-6}$	92	30	10.5
<b>SAL 2%</b>	-	39	62	$5.95 \times 10^{-6}$	93	27	10.1

*a* Obtained from cumulant analysis (standard deviation between brackets)

*b* Measured at 4%

**Table 4.** Structural parameters obtained from SANS for the free and drug-loaded F127 micelles (5%) with added DIMEB in D<sub>2</sub>O at 37°C (1% of all drugs, 0.65% for LD). The scattering data were fitted to a core-shell model interacting through a hard-sphere (HS) structure factor (for the micelles), to which a contribution of spheres of fixed radius (10 Å) was added to model the cyclodextrins.

F127 micelles with:	Core Radius /Å	Shell Thickness /Å	Shell sld /Å <sup>2</sup>	HS volume fraction	Polydispersity core/shell
no drug, 5%DIMEB	42	55	$6.13 \times 10^{-6}$	0.14	0.2/0.2
no drug, 7%DIMEB	37	50	$6.08 \times 10^{-6}$	0.10	0.2/0.2
no drug, 9%DIMEB	28	32	$5.89 \times 10^{-6}$	0.03	0.2/0.2
LD, 11% DIMEB	35	49	$6.03 \times 10^{-6}$	0.11	0.2/0
LD, 13% DIMEB	29	44	$5.96 \times 10^{-6}$	0.07	0.2/0
PB, 9% DIMEB	41	60	$6.20 \times 10^{-6}$	0.15	0.2/0.2
PB, 11% DIMEB	36	59	$6.25 \times 10^{-6}$	0.12	0.3/0
PB, 13% DIMEB	26	54	$6.15 \times 10^{-6}$	0.09	0.25/0
NP, 9% DIMEB	41	60	$6.19 \times 10^{-6}$	0.15	0.2/0.2
NP, 11% DIMEB	33	53	$6.13 \times 10^{-6}$	0.10	0.2/0.2
NP, 13% DIMEB	28	54	$6.14 \times 10^{-6}$	0.10	0.2/0
SAL, 9% DIMEB	35	57	$6.17 \times 10^{-6}$	0.11	0.25/0
SAL, 13% DIMEB	24	35	$6.15 \times 10^{-6}$	-	-

**Table 5.** Drug:CD binding constant  $K/X^{-1}$ (g/g of complex) at 37°C determined using Eq. 3. The concentration of drug is  $C_{\text{drug}} = 10^{-3}$  wt%. The wavelength of the maximum of fluorescence used is shown between brackets where the spectrum presented more than one maximum. The values of K shown between brackets correspond to the values measured at 25°C (reproduced from <sup>1</sup>).

DRUG	$K/X^{-1}$ (g/g)
Lidocaine	$3 \pm 0.1$ (F <sub>290</sub> )/ ( $3.80 \pm 0.1$ )
Pentobarbital	$20 \pm 2$ (F <sub>355</sub> ) /( $48.92 \pm 1.9$ )
Salicylate	$423 \pm 3$ /( $440.9 \pm 30.1$ )
Naproxen	$468 \pm 133$ /( $625 \pm 25$ )

**Table 6.** Binding constant  $K/X^{-1}(\text{g/g})$  of the drugs to F127 Pluronic micelles in a 5 wt% micellar solution at 37°C determined using Eq. 2. Two drugs concentrations are studied: (a) diluted: with  $C_{\text{drug}} = 10^{-3}$  wt% and (b) concentrated:  $C_{\text{drug}} = 2$  wt% (except for lidocaine where  $C_{\text{drug}} = 0.3$  wt%). The cmc values used are given in Table 1. The values measured at 25°C are shown between brackets (reproduced from <sup>1</sup>).

<b>DRUG</b>	<b><math>K/X^{-1}(\text{g/g})</math> Diluted</b>	<b><math>K/X^{-1}(\text{g/g})</math> Concentrated</b>
<b>lidocaine</b>	$9 \pm 0.05$ (F <sub>330</sub> )/(1.50±0.13)	$140 \pm 32$ (F <sub>295</sub> )/(34.5±0.9)
<b>pentobarbital</b>	$10 \pm 2$ (F <sub>340</sub> )/(8.83±0.99)	$1167 \pm 20$ (F <sub>297</sub> )/(7.79±2.0)
<b>naproxen</b>	<i>Not detected</i>	$45.6 \pm 0.5$ /(3.56±0.95)
<b>salicylate</b>	<i>Not detected</i>	$18.3 \pm 0.34$ /(4.67±0.37)

## Figure Captions

**Figure 1:** Small-angle neutron scattering curves from 5% F127 micelles at 37°C with various amounts of the four drugs loaded: **A.** with 0.5, 1 and 2% pentobarbital (inset: same data in a lin-log plot to highlight changes in intensity) with varying drug content); **B.** with 1 and 2% naproxen or salicylate; **C.** as in B, but with curves staggered. **D.** with 0.67% lidocaine.

**Figure 2:** Small-angle neutron scattering curves from 5% F127 micelles with and without the four drugs studied and increasing amounts of DIMEB. Figures on the right-hand-side are the same as on the left hand-side but staggered for better visibility; the left-hand side figures are included to better visualise the overlap of some of the curves. **A.** Comparison between pentobarbital and naproxen: 5% F127 with 5, 7 and 9% DIMEB and the same micelles with either 1% pentobarbital and 9, 11 and 13% DIMEB or 1% naproxen and 9 and 13% DIMEB. **B.** Comparison between naproxen and salicylate: 5% F127 loaded with 1% salicylate or naproxen; 5% F127 micelles with 7% DIMEB and the same micelles with either 1% salicylate or naproxen and 9 and 13% DIMEB. **C.** Comparison of pentobarbital and lidocaine: 5% F127 loaded with either 1% pentobarbital and 0.67% lidocaine and 11 and 13% DIMEB. **D.** As in A but staggered curves. **E.** As in B but staggered curves. **F.** As in C but staggered curves.

**Figure 3.** Change of the fluorescence intensity (circles) and fits to Eq. 3 (solid line) for drugs ( $10^{-3}$ % wt) **A.** in the absence and **B.** presence of 5% F127, at increasing DIMEB concentrations.

**Figure 4:** Change in fluorescence intensity (circles) and fitting to Eq. 2 (solid line): of **A.** 0.3% LD; **B.** 2% PB; **C.** 2% NP and **D.** 2% SAL in the presence of increasing amounts of F127.

**Figure 5:** Small-angle neutron scattering data from 4 wt% F127 micelles with drug, either **A.** 1% PB or **B.** 1% NP, in the presence of 5% DIMEB at different time points after mixing: 0.1 s, 1.5 s, 111.1 s, 622.1 s, and 642.1 s at 25°C.

**Scheme 1.** Chemical structure of lidocaine, sodium pentobarbital, naproxen sodium salt, and sodium salicylate.

**Scheme 2:** Solubilisation locus of the drugs in the polymeric micelles as inferred from a combination of SANS, UV spectroscopy and 2D NMR as described in the text.

**Figure 1.**

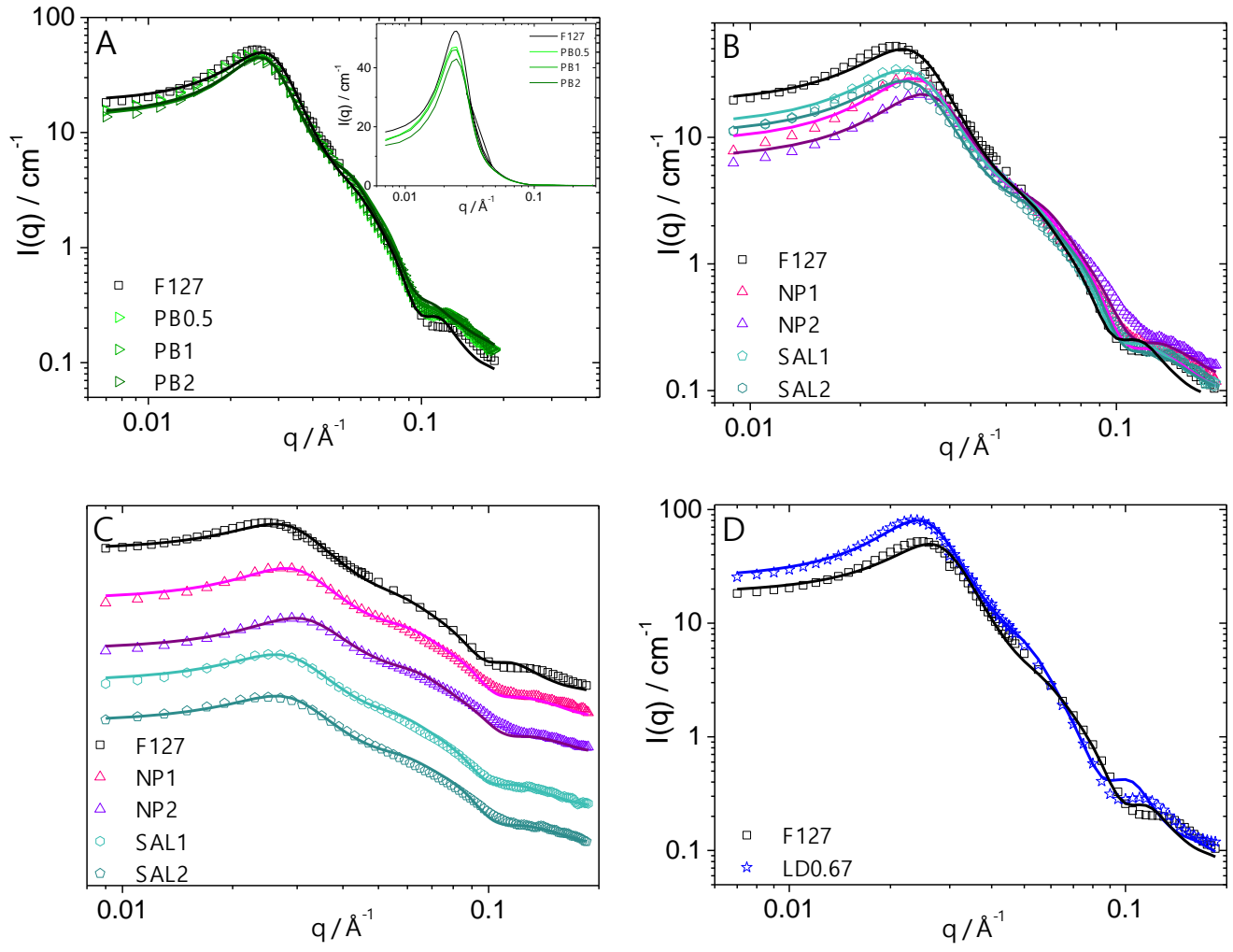




**Figure 2.**

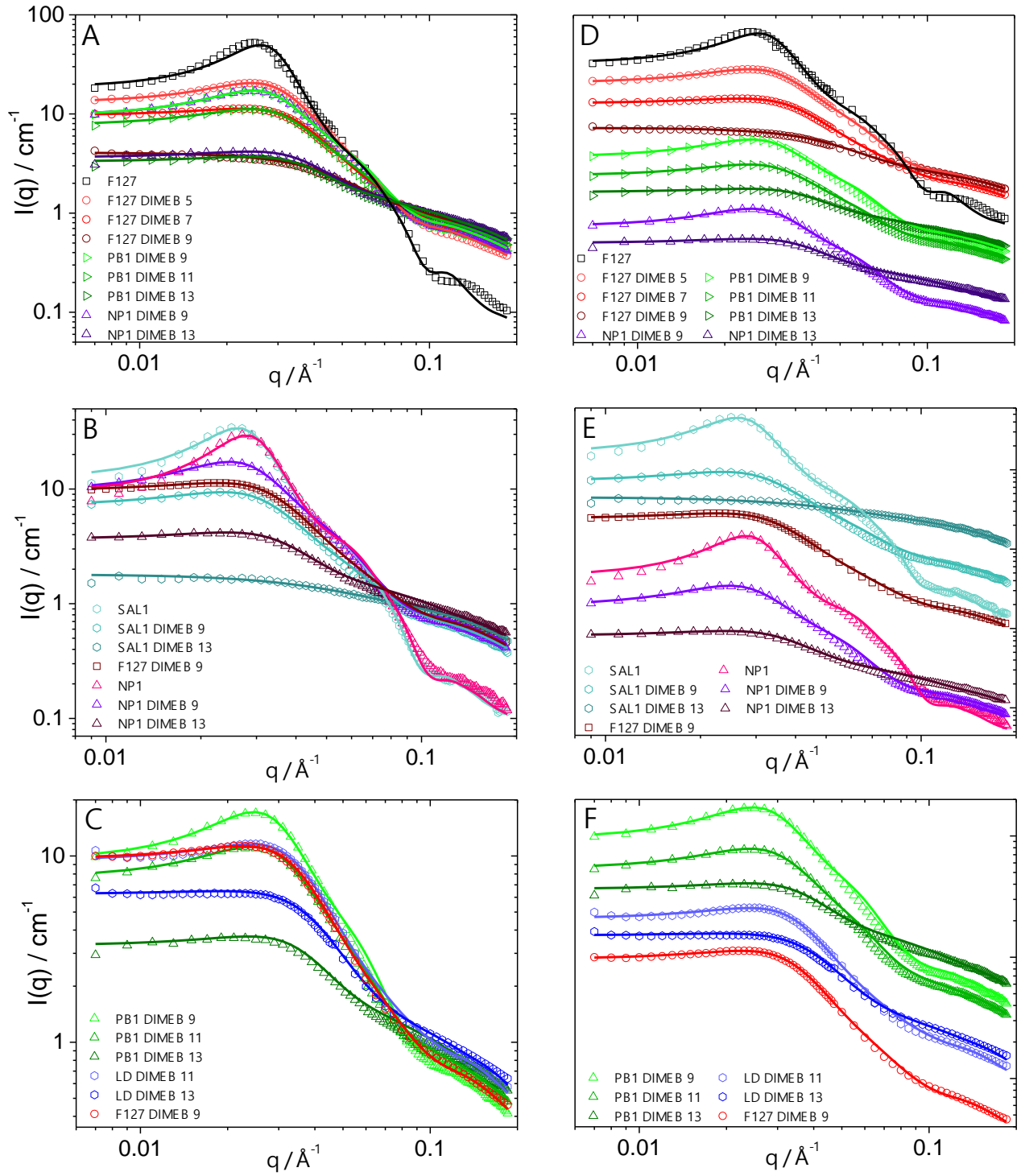
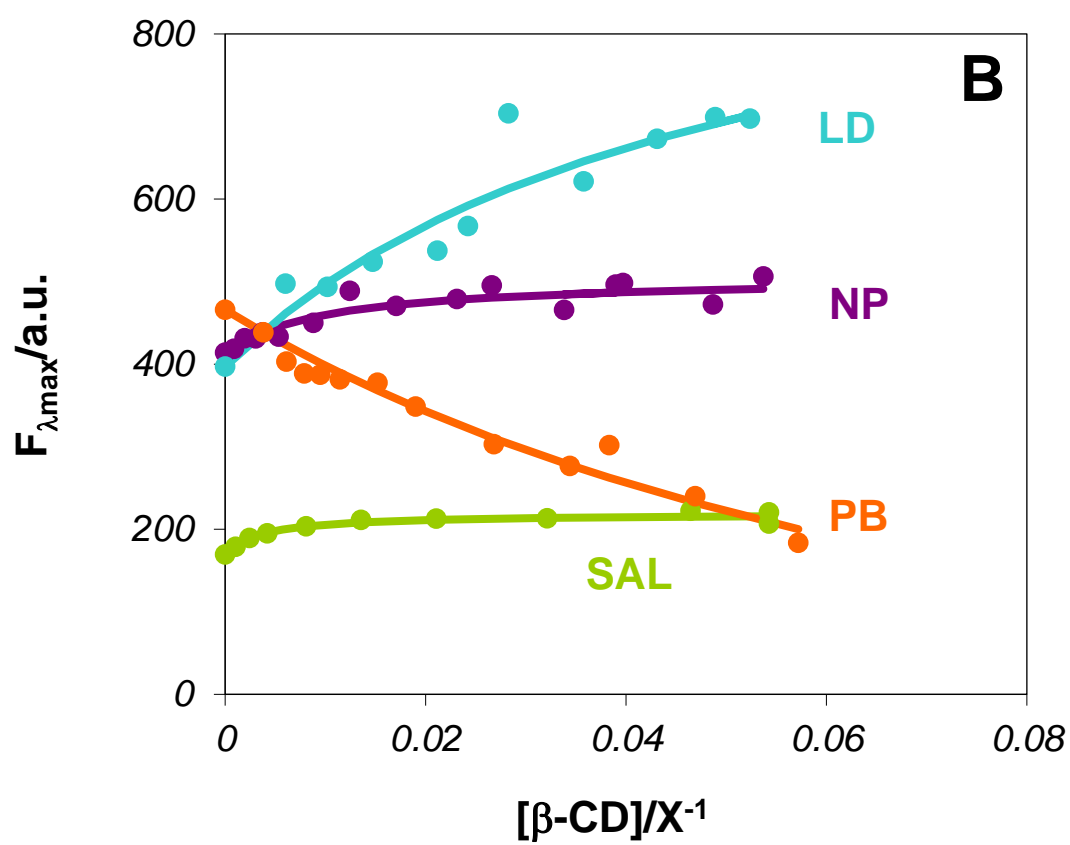
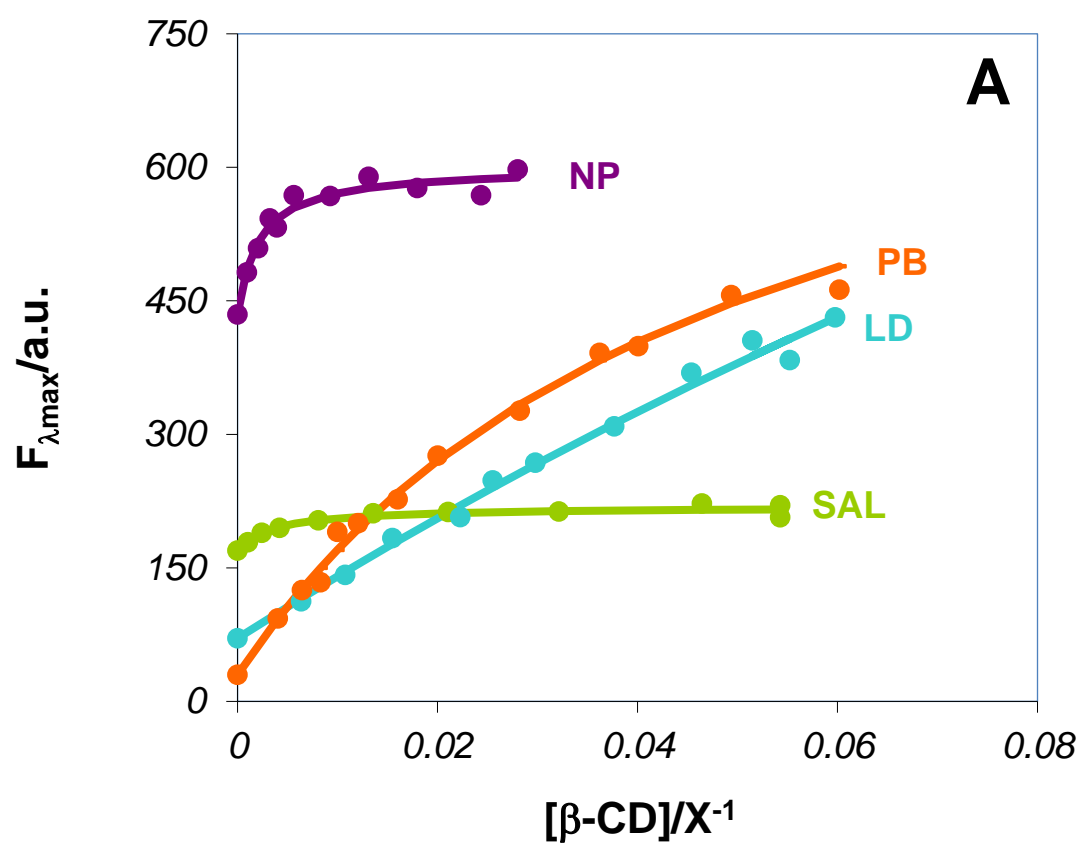
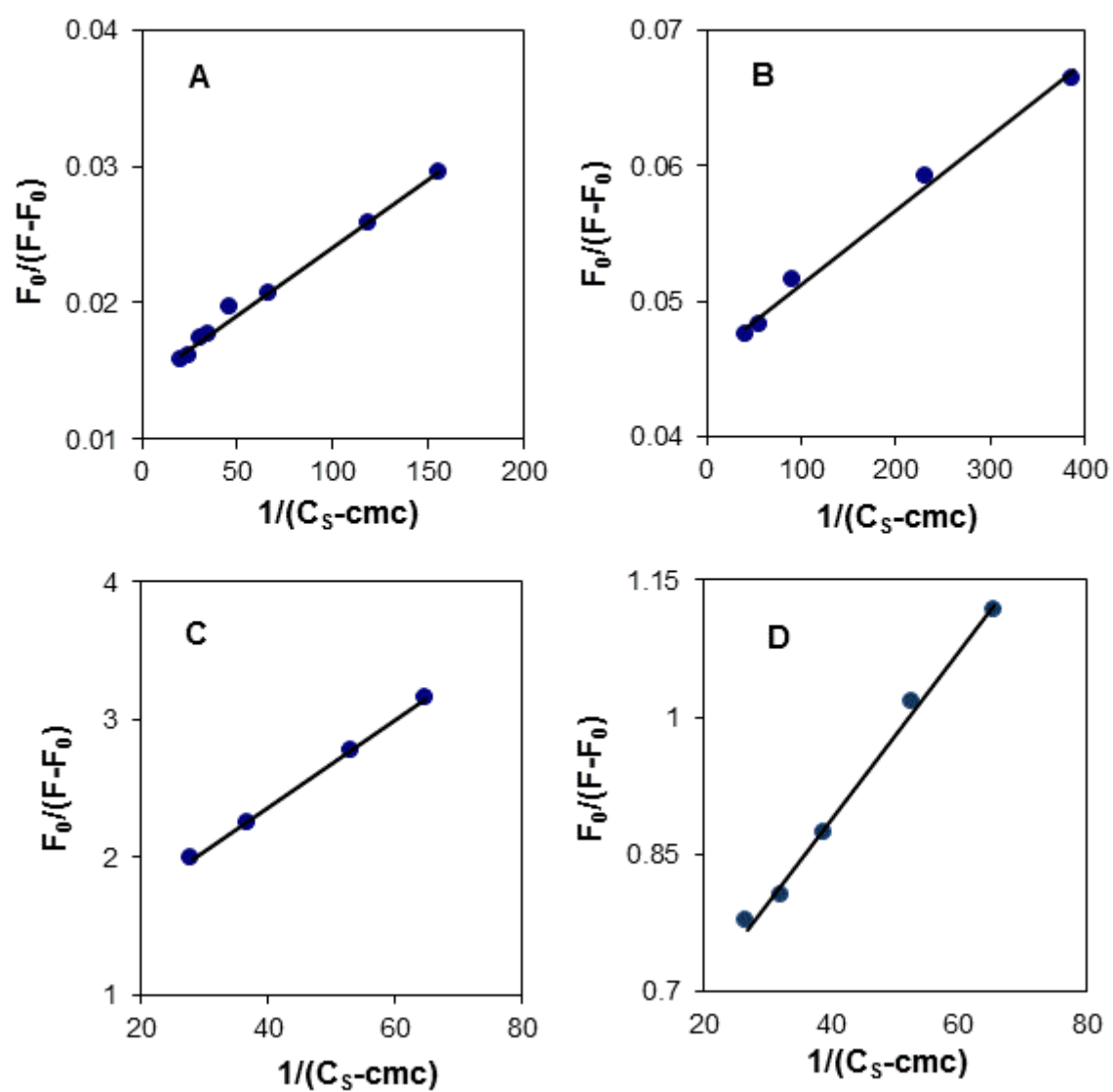


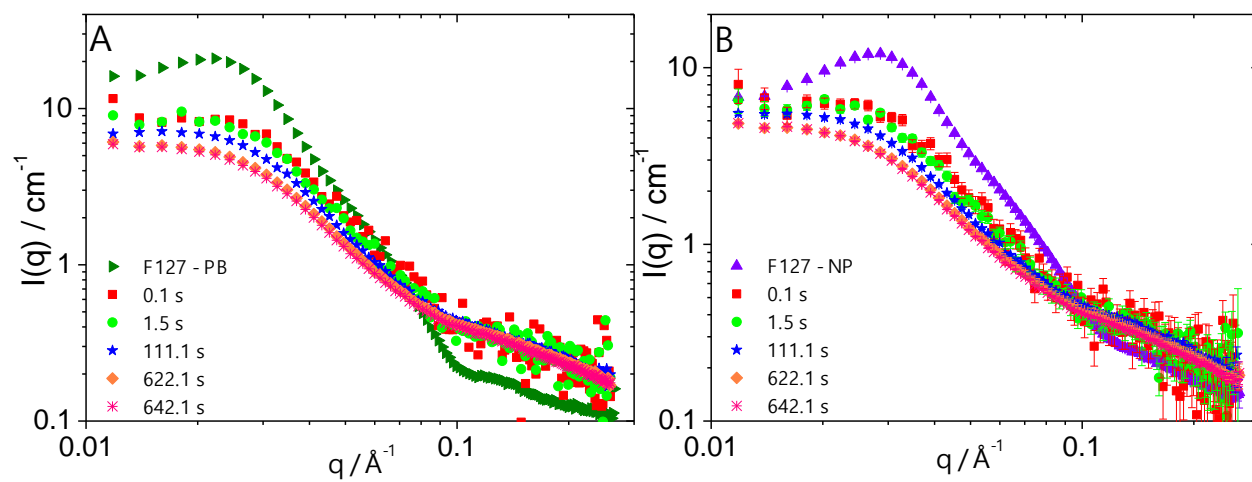
Figure 3.



**Figure 4.**

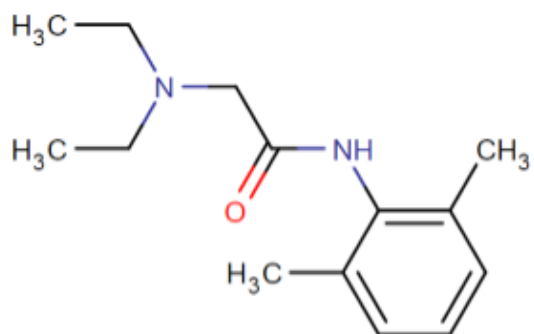


**Figure 5.**

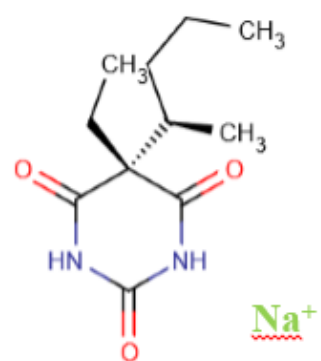


**Scheme 1.**

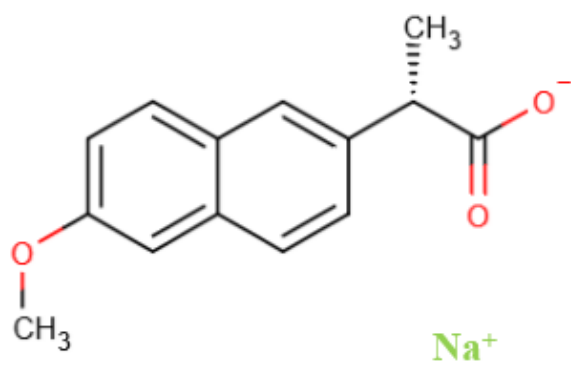
Lidocaine



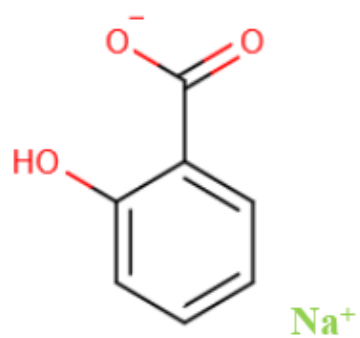
Sodium Pentobarbital



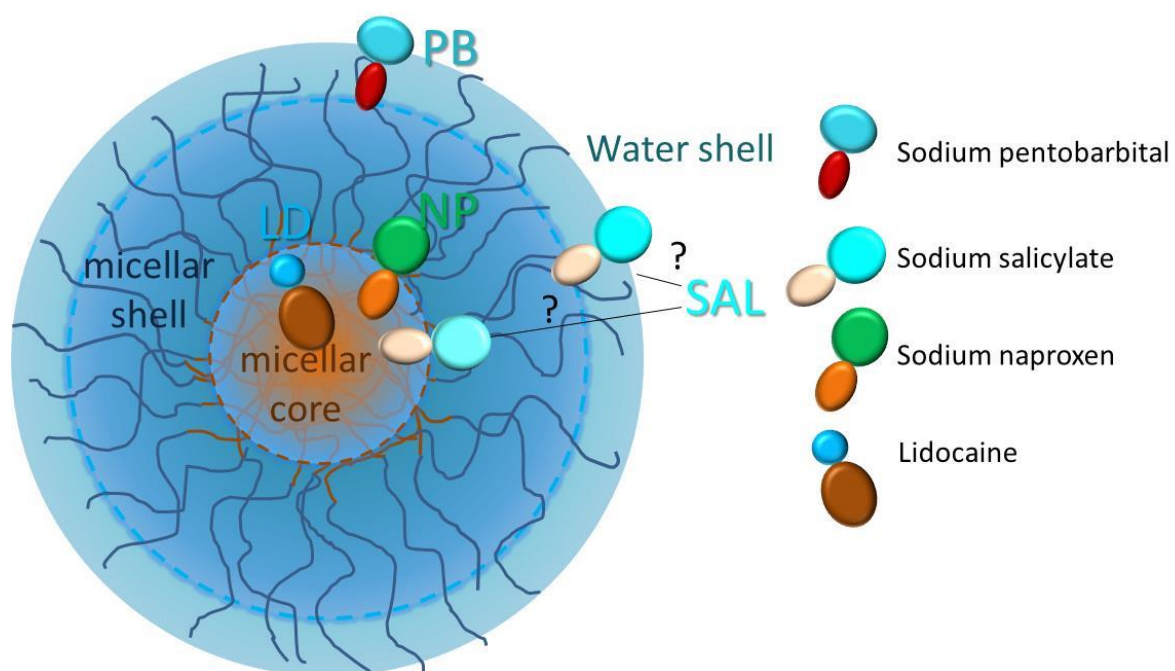
Naproxen Sodium Salt



Sodium Salicylate



**Scheme 2**



For Table of Contents Only

